Nanoscale

PAPER

View Article Online
View Journal | View Issue

Cite this: *Nanoscale*, 2016, **8**, 17815

Thermal conductivity of disordered two-dimensional binary alloys

Yang Zhou,[a,b] Zhi-Xin Guo,[c] Hai-Yuan Cao,[a,b] Shi-You Chen,[a,b] Hong-Jun Xiang[a,b] and Xin-Gao Gong*[a,b]

Received 8th June 2016,
Accepted 7th September 2016

DOI: 10.1039/c6nr04651g

www.rsc.org/nanoscale

Using non-equilibrium molecular dynamics simulations, we have studied the effect of disorder on the thermal conductivity of two-dimensional (2D) $C_{1-x}N_x$ alloys. We find that the thermal conductivity not only depends on the substitution concentration of nitrogen, but also strongly depends on the disorder distribution. A general linear relationship is revealed between the thermal conductivity and the participation ratio of phonons in 2D alloys. Localization mode analysis further indicates that the thermal conductivity variation in the ordered alloys can be attributed to the number of inequivalent atoms. As for the disordered alloys, we find that the thermal conductivity variation can be described by a simple linear formula with the disorder degree and the substitution concentration. The present study suggests some general guidance for phonon manipulation and thermal engineering in low dimensional alloys.

1. Introduction

Thermal conductivity of 2D materials has gained increasing attention in recent years because of their great potential applications in both microelectronics and thermoelectrics. The fast development cycle in the electronic industry leads to a rapid decrease of the size of electronic devices,[1] which makes the dissipation of heat one of the main problems to be addressed.[2] 2D materials may serve as both devices and dissipation paths.[2–5] For example, graphene, a single layer of carbon atoms in a hexagonal lattice, is found to possess not only outstanding electronic properties,[6] but also thermal conductivity as high as 5000 W m^{-1} K^{-1}.[7] Many other monolayer structures have also been found recently and the experimental results on two-dimensional semiconductors are encouraging.[8–14] Some 2D semiconductors also have exceptional thermoelectric properties. Very recently, a large value of the thermoelectric Seebeck coefficient for single-layer MoS_2 was experimentally observed between -4×10^2 and -1×10^5 μV K^{-1}, proving its promising role in thermopower generation.[8] Another example is the greatly enhanced ZT figure of merit value of monolayer phosphorene, which is much larger than that of bulk black phosphorus.[9] Since disorder defects are unavoidable in real materials, understanding the nature of their effect on thermal conductivity is important for the development of microelectronics and thermoelectrics.

Lattice defects, which are unavoidable in real materials, may drastically change the thermal properties.[10–12] For example, it has been widely reported that the thermal conductivity of disordered three-dimensional (3D) alloys is much lower than that of the constituent pure solids.[13–18] The virtual crystal approximation (VCA), which considers mass disorder as a perturbation and the variance of mass as the only factor that influences the phonon scattering rate and other quantities, has also been proposed and experimentally verified[14] in understanding the thermal conductivity of random 3D alloys. Recently, Baker *et al.* further explored the effect of long and short range orders on the thermal conductivity of SiGe alloys,[19] and they found that the thermal conductivity is almost entirely determined by the nearest-neighbor short-range order in the alloy. Relaxation-time calculations showed that ordering can increase the thermal conductivity due to the reduction of disorder-induced anharmonic phonon scattering.[19]

Despite the well explored thermal conductivity of disordered 3D alloys, similar investigations of 2D disordered alloys are far from complete. It has been found that 2D materials exhibit very different thermal conduction properties from 3D materials due to 2D quantum confinement effects on phonon transport.[20] This implies the possible existence of new mechanisms of disorder effects on the thermal conductivity of 2D materials.

[a]*Key Laboratory for Computational Physical Science (Ministry of Education), State Key Laboratory of Surface Physics and Department of Physics, Fudan University, Shanghai 200433, China. E-mail: xggong@fudan.edu.cn*
[b]*Collaborative Innovation Center of Advanced Microstructures, Nanjing 210093, Jiangsu, China*
[c]*Department of Physics, Xiangtan University, Xiangtan 411105, China*

In this work, through a systematic investigation of the thermal conductivity of $C_{1-x}N_x$ 2D alloys with various substitutional disorders, we reveal the mechanism of how disorder affects the thermal conductivity. Unlike the disordered alloys, whose thermal conductivity can be effectively described using the mass-disorder perturbation model. Our results show that the thermal conductivity of 2D alloys also strongly depends on the distribution of the substitution atoms. We propose a phenomenological linear expression which directly estimates the thermal conductivity of disordered 2D alloys through the structure order parameter.

2. Computational details

We employ the non-equilibrium molecular dynamics (NEMD) method which is implemented in the LAMMPS.[21] Thermal conductivity is defined by the Fourier formula:

$$\kappa = \frac{\langle J_x \rangle}{\langle \nabla T \rangle}, \quad (1)$$

where ∇T is the temperature gradient along the heat conduction direction from a least squares fit, and $J_x = \frac{h}{\Delta t S}$ is the heat flux obtained from the Nosé–Hoover work h and crossover area S. The angular bracket denotes an ensemble average, and Δt is the MD timestep parameter.

In the simulation, the periodic boundary condition is applied in the transverse direction, and the free boundary condition is applied in the other two directions. For each simulation, all the atoms are initially placed at their equilibrium positions at zero pressure. Then the two ends are fixed to eliminate bulk translation and rotation.[22] The atoms in the unfixed interior possess random Gaussian distributed velocities, which are then equilibrated at T = 300 K with the Nosé–Hoover thermostat[15] for 2×10^5 steps of 0.1 ns. After that, the temperature difference is established using two Nosé–Hoover heat baths of 290 K and 310 K, respectively, in the two regions behind the fixed region for other 1×10^7 steps of 5.0 ns to drive the system to a stable temperature and heat flux distributions. Finally, the thermal conductivity is calculated from eqn (1). The final result is averaged over 5 simulations with different initial conditions. The calculation configuration is indicated in Fig. 1a.

Various simulation cells were constructed to explore the substitution concentration and the distribution dependence of thermal conductivity. Typical views of the unit cells of $C_{12}N$, C_3N [23] and CN, respectively, are shown in Fig. 1b–d. The cell is rectangular as required by NEMD. Each has the dimensions of 17.84 Å × 31.19 Å and includes 208 atoms. They are large enough in the transverse direction and size-confinement effects can be ignored. The structure of $C_{1-x}N_x$ is initially the graphene structure with 22 × 1 × 1 rectangular unit cells in the x, y, and z directions, respectively.

The BCN Tersoff potential[24] is used because it accurately describes the elastic properties. In the BCN potential, both two-body and three-body terms are considered so there is a stable graphene-like structure. The velocity Verlet algorithm[25] is employed to integrate Newton's equations of motion. The overall trends of our results are verified by NEMD simulations using the Müller-Plathe method.[26]

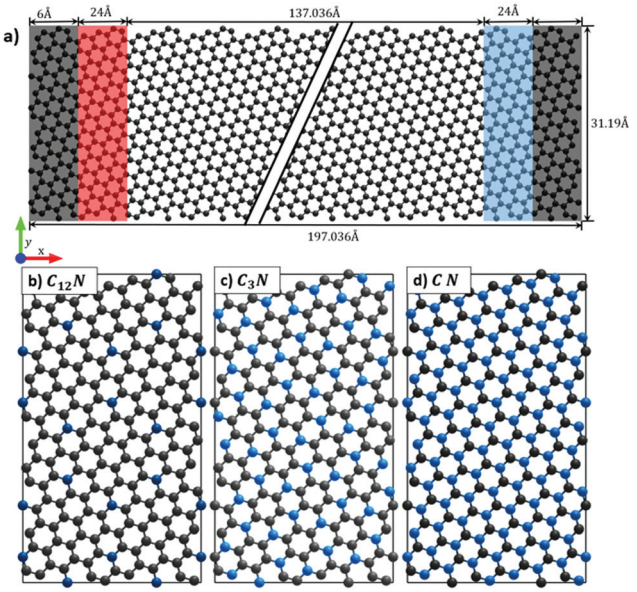

Fig. 1 (a) The simulation configuration in our NEMD simulations. The system used contains 22 × 1 × 1 unit cells, where the gap is used to represent the repeating units. The periodic boundary condition is applied in the y direction and free boundary conditions are applied in the x and z directions. The outmost two ends (shown as grey) are fixed after optimizing the system under zero pressure. The next two unit cells (shown as red on the left and blue on the right) are heated by the Nosé–Hoover thermostat at the temperatures of 310 K and 290 K, respectively. (b)–(d) Show the unit cells of the $C_{12}N$, C_3N, and CN ordered alloys, respectively, where carbon is black and nitrogen is blue. Each unit cell is rectangular and consists of 208 atoms.

3. Results and discussion

The thermal conductivity of random alloys is very sensitive to the substitution concentration. Fig. 2a shows the calculated thermal conductivity of $C_{1-x}N_x$ at 300 K. As one can see, a 1% substitution of nitrogen induces a 35% reduction of thermal conductivity for the usual random alloys. The thermal conductivity further decreases to below 5% of its original value when the substitution concentration reaches 20%, beyond which the structure becomes unstable. As for alloys with an ordered distribution of nitrogen, the thermal conductivity shows a rather different trend. It does not decrease much while the substitution concentration increases, but it increases as the ratio goes beyond 1/13. For a given substitution concentration, the ordered structure shows the largest thermal conductivity and any disordering decreases the thermal conductivity. As the disordering becomes completely random, the thermal conductivity reaches a minimum.

The thermal conductivity is closely correlated with the energetics of different $C_{1-x}N_x$ structures. In Fig. 2b we show the

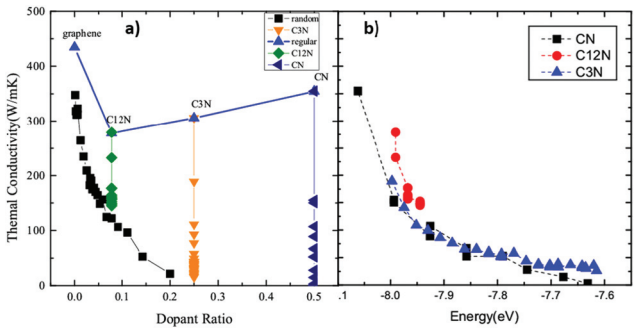

Fig. 2 The substitution concentration and the distribution dependence of thermal conductivity. (a) Thermal conductivity of $C_{1-x}N_x$ with different distributions *versus* substitution concentration at 300 K. The thermal conductivities of random alloys are shown as black solid squares and ordered alloys as blue solid triangles. The remaining three lines paralleling the *y* axis represent the thermal conductivity of structures with the same ratio but different disorder distributions (called disordered alloys). It is found that thermal conductivity is sensitive to both substitution concentration and distribution. (b) The total energy dependence of the thermal conductivity of disordered alloys shown in (a). For a given substitution concentration, the more stable structure always has a higher thermal conductivity.

calculated total energy (eV per atom) dependence of thermal conductivity of various disordered $C_{1-x}N_x$ structures. It is seen that with the same nitrogen substitution concentration, the thermal conductivity monotonically decreases with the increase of total energy. This shows that the alloys with a similar total energy have similar thermal conductivities, and the more stable structures have higher thermal conductivities in the disordered 2D alloys, independent of the substitution concentration. This also shows that the concentration is not the only major factor influencing the thermal conductivity of 2D alloys. To quantitatively describe the thermal conductivity variation, we have to include the effect of disorder distributions, which can be described by the structure order parameter.

Mode localization of phonons is believed to be responsible for the disorder distribution dependence of thermal conductivity. To understand the underlying physical mechanism of the thermal conductivity variation of $C_{1-x}N_x$ alloys in Fig. 2a, we first carry out a vibrational eigen-mode analysis of the ordered alloys. The mode localization can be quantitatively characterized by the participation ratio[27] $P_{k\sigma}$ for each eigen-mode kσ,

$$P_{k\sigma} = \frac{1}{N\sum_s \left(\varepsilon^*_{k\sigma}(s)\varepsilon_{k\sigma}(s)\right)^2}, \quad (2)$$

Here N is the total number of atoms and $\varepsilon_{k\sigma}(s)$ is the complex amplitude of atom s for eigen-mode kσ. The participation ratio represents the fraction of atoms participating in a given mode, which effectively indicates the localized phonon modes with $O\left(\frac{1}{N}\right)$ and delocalized phonon modes with O (1). Thus, it provides detailed information about the localization effect of each phonon mode.

We calculate the eigen vectors and frequencies using Phonopy[28] with a 4 × 4 × 1 supercell and 31 × 31 × 1 mesh sampling. Fig. 3 shows the participation ratios of graphene, C_3N, $C_{12}N$ and CN ordered alloys, respectively. For graphene, all the phonon modes, as expected, are essentially delocalized. In the CN alloy, only a few modes are partially localized. While for the $C_{12}N$ and C_3N, a considerable number of phonon modes become localized and the participation ratio of some modes becomes very small. We find that such a participation ratio is closely correlated with the thermal conductivity as shown in Fig. 2a. The average participation ratios are 1.00, 0.80, 0.86 and 0.95 for graphene, C_3N, $C_{12}N$ and CN, respectively, which obey the same trends as the thermal conductivity $\kappa_{graphene} > \kappa_{CN} > \kappa_{C_3N} > \kappa_{C_{12}N}$. Fig. 4 further displays the relationship between the thermal conductivity and the average participation ratio for various ordered alloys, where a roughly linear relationship was found. This means that the structure variation influences the thermal conductivity directly *via* the average phonon participation ratio. The linear relationship between the thermal conductivity and the average participation ratio verifies the assertion that if the phonons are more nonlocalized, the solid would be more thermally conductive.

Although the participation ratio can describe the mode localization in a quantitative manner, it cannot provide detailed information about the spatial distribution of a specific mode. To get a better understanding of the localiz-

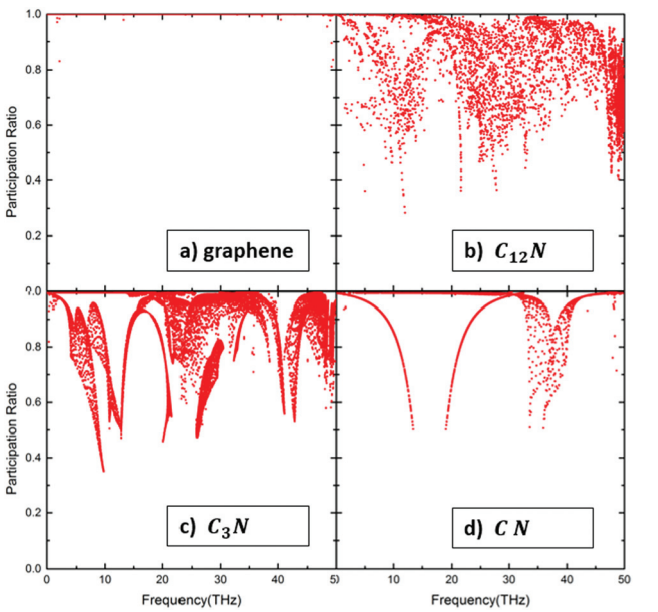

Fig. 3 Participation ratio *versus* phonon frequency for (a) graphene, (b) $C_{12}N$ ordered alloy, (c) C_3N ordered alloy, and (d) CN ordered alloy. Each point represents a phonon mode labeled by ($\vec{k}$, σ) where $\vec{k}$ is the wave vector and σ is the phonon branch. Nearly all the phonon modes in graphene are delocalized, which corresponds to the surprisingly large thermal conductivity. In the CN alloy, only a few modes are partially localized. While for the $C_{12}N$ and C_3N, a considerable number of phonon modes become localized, and the participation ratio of some modes becomes very small.

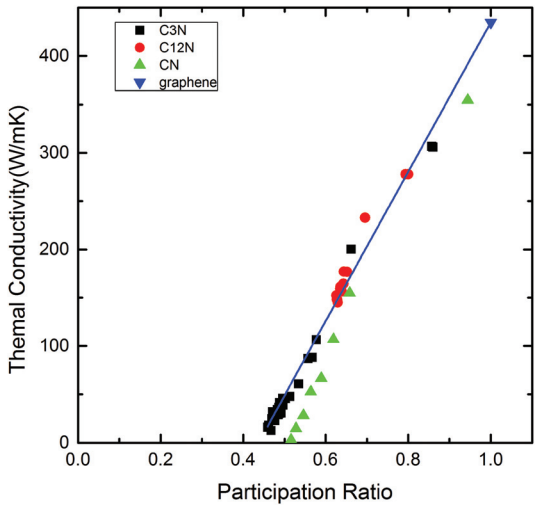

Fig. 4 Thermal conductivity *versus* average participation ratio of graphene and different ordered alloys. The linear relationship between thermal conductivity and participation ratio is obtained for all substitution concentrations and distributions.

ation modes, we present the spatial vibration strength distribution of a typical mode of ordered C_3N in Fig. 5a. As we can see, with the presence of nitrogen atoms, carbon atoms are grouped into three classes under the operation of translation and inversion. So we can define the inequality number of atom N_e for each structure. The N_e of graphene, C_3N, $C_{12}N$ and CN is 1, 4, 7, and 2, respectively. Fig. 5b shows the relationship between the thermal conductivity and the reciprocal of N_e for the four ordered structures. One can see that the presence of the substitution atoms increases the inequality number of the atoms, and thus decreases the thermal conductivity. This is

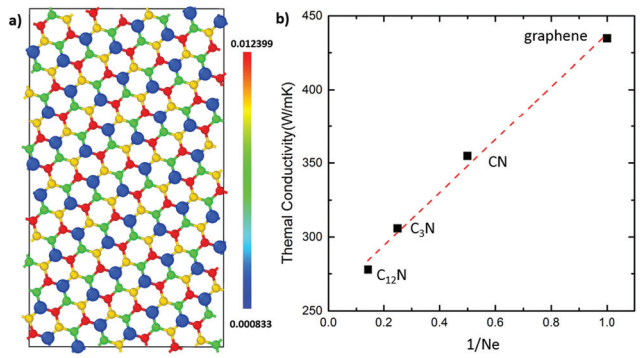

Fig. 5 (a) The vibrational amplitude spatial distribution of a typical phonon mode of C_3N. The blue balls correspond to nitrogen atoms, which are enlarged as a guide to the eye. The vibration of carbon atoms can be classified into three classes, shown as red, green and yellow balls. This result suggests that we define the inequality according to the symmetry under translation and inversion operator. The presence of periodic nitrogen atoms modulates the vibration of carbon atoms and causes the localized phonons. (b) Thermal conductivity *versus* reciprocal inequality number of graphene, $C_{12}N$, C_3N, and CN ordered alloys. The presence of the substitution atoms increases the inequality number of the atoms, and thus decreases the thermal conductivity.

because increasing the inequality number of atoms in the ordered alloys increases the phonon interference, which is responsible for the decrease of thermal conductivity. Qualitatively this is because the more the inequality number of atoms, the larger the phonon scattering and thus the thermal resistance.

In the disordered alloys, almost all the atoms are not equivalent, which makes them unsuitable for defining the inequality number of atoms. So we have to find another way to quantitatively define the structural disorder which is directly related to thermal conductivity. Here, we define a structure-determined disorder degree d as:

$$d = \frac{1}{r_c}\int_0^{r_c} \frac{\Delta g(r)}{g(r)}\mathrm{d}r, \tag{3}$$

where

$$g(r) = \frac{1}{N_0}\sum_i g_i(r), \tag{4}$$

is the average pair correlation function of nitrogen atoms $g_i(r)$,[29] and N_0 is the number of nitrogen atoms. Now we use:

$$\Delta g(r) = \sqrt{\frac{1}{N_0}\sum_i (g_i(r) - g(r))^2}, \tag{5}$$

as the standard error of $g_i(r)$. In other words, the disorder degree d is a measure of the average relative error of the pair correlation function of alloying atoms. For the ordered alloys, obviously d is zero. Also, for a large enough r_c, $\Delta g(r) \to 0$ because $g_i(r) \to 1$, so that d converges. Since $g_i(r)$ reflects the environment of atom i, the large relative error d corresponds to a stronger disorder. Thus, d is a good parameter describing the disorder in the alloy.

In Fig. 6a, we show the disorder degree (d) dependence of thermal conductivity for the C_3N, $C_{12}N$ and CN alloys, where the linear relationship is obtained for all three alloys, *i.e.*, the thermal conductivity monotonically decreases with the increase in the disorder degree. For a given substitution ratio of nitrogen, the ordered alloy (d = 0) always has the largest thermal conductivity as expected. Also, the slope of the line is proportional to the substitution concentration. So we arrived at a simple relationship, *i.e.*, the thermal conductivity is proportional to $r \times d$, where r is the substitution concentration. As shown in Fig. 6b, nearly the same linear dependence of thermal conductivity on $r \times d$ is obtained for different $C_{1-x}N_x$ alloys, which may be a universal scaling for 2D alloys. To use this relationship, we can easily evaluate the thermal conductivity of an alloy with only the knowledge of several points on the line. Also, it helps us to connect thermal conductivity and electric conductivity *via* the disorder degree, which is helpful to find better thermoelectric materials. Although disorder can simultaneously affect both thermal and electronic conductivities, one can find a maximum if the electronic conductivity follows a different relationship instead of a linear relationship.

Our proposed order parameter d is a different order parameter from the often mentioned η,[30] but they must be

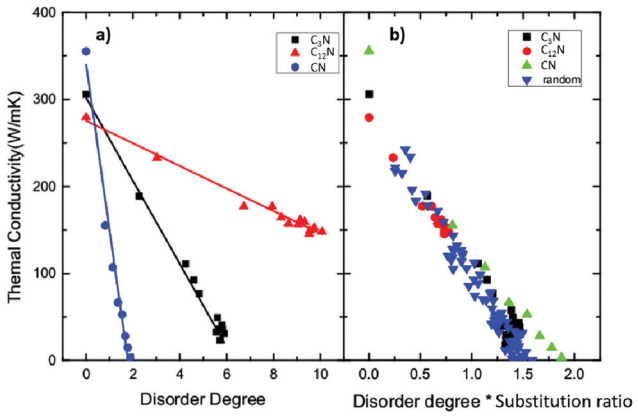

Fig. 6 Thermal conductivity *versus* disorder degree for the $C_{12}N$, C_3N, and CN alloys. The thermal conductivity almost linearly depends on the disorder degree. The slopes of the lines strongly depend on the substitution concentration. (b) Thermal conductivity *versus* the product of disorder degree and substitution concentration, which shows a linear relationship. The effects of substitution concentration on the slope of the lines shown in (a) can be seen in (b).

somehow related to each other. The key difference is that the η is an order parameter with a reference of an ordered structure, while the parameter d proposed in the present manuscript does not have any reference ordered structure.

4. Conclusions

In this work, we have systematically studied the effect of substitution disorder on the thermal conductivity of $C_{1-x}N_x$ 2D alloys. In contrast to 3D alloys, the thermal conductivity of which can be effectively described by using the mass-disorder perturbation model, we have found that the thermal conductivity of 2D alloys not only depends on the substitution concentration but also strongly depends on the degree of the disorder distribution. The number of the inequivalent atoms is responsible for the variation of thermal conductivity in the ordered alloys. As for the disordered 2D alloys, we have found that the thermal conductivity variation can be well described by a linear relationship with the product of disorder degree and substitution concentration. Our study is expected to be valuable for the thermal conductivity manipulation in 2D alloys.

Acknowledgements

This paper was partially supported by the National Natural Science Foundation of China, the Special Funds for Major State Basic Research, the Foundation for the Author of National Excellent Doctoral Dissertation of China, the Program for Professor of Special Appointment at Shanghai Institutions of Higher Learning, and the Research Program of Shanghai Municipality and the Ministry of Education. Z. X. acknowledges support from the Natural Science Foundation of Hunan Province (No. 2015JJ6106).

Notes and references

1 R. R. Schaller, *IEEE Spectrum*, 1997, **34**, 52–59.
2 R. Mas-Ballesté, C. Gómez-Navarro, J. Gómez-Herrero and F. Zamora, *Nanoscale*, 2011, **3**, 20–30.
3 J. Y. Kim, J.-H. Lee and J. C. Grossman, *ACS Nano*, 2012, **6**, 9050–9057.
4 S. Chen, Q. Wu, C. Mishra, J. Kang, H. Zhang, K. Cho, W. Cai, A. A. Balandin and R. S. Ruoff, *Nat. Mater.*, 2012, **11**, 203–207.
5 J. Lan and B. Li, *Phys. Rev. B: Condens. Matter*, 2006, **74**, 054305.
6 K. S. Novoselov, A. K. Geim, S. V. Morozov, D. Jiang, M. I. Katsnelson, I. V. Grigorieva, S. V. Dubonos and A. A. Firsov, *Nature*, 2005, **438**, 197–200.
7 A. A. Balandin, S. Ghosh, W. Bao, I. Calizo, D. Teweldebrhan, F. Miao and C. N. Lau, *Nano Lett.*, 2008, **8**, 902–907.
8 X. Song, J. Hu and H. Zeng, *J. Mater. Chem. C*, 2013, **1**, 2952.
9 H. Y. Lv, W. J. Lu, D. F. Shao and Y. P. Sun, *Phys. Rev. B: Condens. Matter*, 2014, **90**, 085433.
10 Y. Lee, S. Lee and G. S. Hwang, *Phys. Rev. B: Condens. Matter*, 2011, **83**, 125202.
11 N. A. Katcho, J. Carrete, W. Li and N. Mingo, *Phys. Rev. B: Condens. Matter*, 2014, **90**, 094117.
12 B. Abeles, *Phys. Rev.*, 1963, **131**, 1906–1911.
13 J. Garg, N. Bonini, B. Kozinsky and N. Marzari, *Phys. Rev. Lett.*, 2011, **106**, 045901.
14 C. Y. Ho, M. W. Ackerman, K. Y. Wu, S. G. Oh and T. N. Havill, *J. Phys. Chem. Ref. Data*, 1978, **7**, 959–1178.
15 A. J. C. Ladd, B. Moran and W. G. Hoover, *Phys. Rev. B: Solid State*, 1974, **34**, 5058–5064.
16 S. Adachi, *J. Appl. Phys.*, 1985, **58**, R1–R29.
17 B. Abeles, D. Beers, G. Cody and J. Dismukes, *Phys. Rev.*, 1962, **125**, 44–46.
18 B. Abeles, *Phys. Rev.*, 1963, **131**, 1906–1911.
19 C. H. Baker and P. M. Norris, *Phys. Rev. B: Condens. Matter*, 2015, **91**, 180302.
20 D. L. Nika and A. A. Balandin, *J. Phys.: Condens. Matter*, 2012, **24**, 233203.
21 S. Plimpton, *J. Comput. Phys.*, 1995, **117**, 1–19.
22 Z. Guo, D. Zhang and X. G. Gong, *Appl. Phys. Lett.*, 2009, **95**, 163103.
23 H. J. Xiang, B. Huang, Z. Y. Li, S. H. Wei, J. L. Yang and X. G. Gong, *Phys. Rev. X*, 2012, **2**, 011003.
24 A. KInacI, J. B. Haskins, C. Sevik and T. ÇağIn, *Phys. Rev. B: Condens. Matter*, 2012, **86**, 115410.
25 J. M. Dickey and A. Paskin, *Phys. Rev.*, 1969, **188**, 1407–1418.
26 F. Müller-Plathe, *Phys. Rev. E: Stat. Phys., Plasmas, Fluids, Relat. Interdiscip. Top.*, 1999, **59**, 4894–4898.
27 L. Yang, N. Yang and B. Li, *Sci. Rep.*, 2013, **3**, 1143.
28 A. Togo, F. Oba and I. Tanaka, *Phys. Rev. B: Condens. Matter*, 2008, **78**, 134106.
29 M. Bishop, *Am. J. Phys.*, 1984, **52**, 1106.
30 S.-H. Wei, D. B. Laks and A. Zunger, *Appl. Phys. Lett.*, 1993, **62**, 1937.